

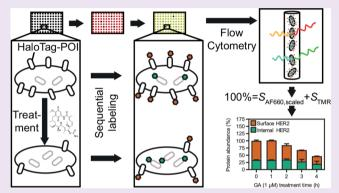
# High-Throughput Quantification of Surface Protein Internalization and Degradation

Jakob C. Stüber, Florian Kast, and Andreas Plückthun\*

Department of Biochemistry, University of Zurich, Winterthurerstrasse 190, CH-8057 Zurich, Switzerland

Supporting Information

ABSTRACT: Cell surface proteins are key regulators of fundamental cellular processes and, therefore, often at the root of human diseases. Thus, a large number of targeted drugs which are approved or under development act upon cell surface proteins. Although down-regulation of surface proteins by many natural ligands is well-established, the ability of drug candidates to cause internalization or degradation of the target is only recently moving into focus. This property is important both for the pharmacokinetics and pharmacodynamics of the drug but may also constitute a potential resistance mechanism. The enormous numbers of drug candidates targeting cell surface molecules, comprising small molecules, antibodies, or alternative protein scaffolds, necessitate



methods for the investigation of internalization and degradation in high throughput. Here, we present a generic highthroughput assay protocol, which allows the simultaneous and independent quantification of internalization and degradation of surface proteins on a single-cell level. Because we fuse a HaloTag to the cell surface protein of interest and exploit the differential cell permeability of two fluorescent HaloTag ligands, no labeling of the molecules to be screened is required. In contrast to previously described approaches, our homogeneous assay is performed with adherent live cells in a 96-well format. Through channel rescaling, we are furthermore able to obtain true relative abundances of surface and internal protein. We demonstrate the applicability of our procedure to three major drug targets, EGFR, HER2, and EpCAM, examining a selection of well-investigated but also novel small molecule ligands and protein affinity reagents.

umerous cell surface proteins transfer external stimuli to the inside of cells and are therefore essential for regulation of cell phenotype, differentiation, or proliferation. This explains their pivotal role in many diseases, if dysregulated, and justifies the high interest in targeting the relevant surface protein(s) to treat these diseases. Furthermore, receptor internalization and down-regulation are well-established negative feedback mechanisms for natural ligands of surface receptors.

Characterization of drug candidates targeting surface proteins with respect to their effect on internalization and degradation is fundamental to understanding their in vivo efficacies. For an antibody, strong induction of internalization and degradation may be essential for its activity as a signaling antagonist<sup>1,2</sup> or for an antibody drug conjugate (ADC)<sup>3</sup> but is undesired for antibodies engaging Fc receptors for antibodydependent cytotoxicity (ADCC) or bispecific antibodies engaging in immune cell recruitment.4 The receptor fate will also be measured more frequently because many targets cannot be effectively hit with the conventional IgG format, and thus novel formats and mechanisms of action are required. Likewise, many small molecules acting as receptor ligands are of outstanding pharmacological relevance<sup>6</sup> and modulate signaling as well as cellular localization of their cognate receptors, for example, G-protein-coupled receptors (GPCRs).

Interest in selective target down-regulation as a therapeutic strategy was further sparked by the FDA approval of fulvestrant, a selective estrogen receptor degrader. Additionally, pharmacokinetics and -dynamics will always be significantly affected if a drug triggers target internalization and remains bound to its target during this process. Therefore, the interest in measuring such extended biochemical properties of artificial ligands, beyond epitope and affinity, is growing.

Today, hundreds of drug candidates are routinely identified in screenings. However, their biophysical and biological characterization remains a major bottleneck. Whereas for drug-target interactions various assays have been developed over the years to support high-throughput applications, to our knowledge, no such assay is available to follow internalization and degradation at the same time with single-cell resolution. Classical assays quantifying internalization and degradation were based on radioactive labels,8 where noninternalized ligands are removed by acid washing, which appears unsuitable for routine high-throughput application. Newer protocols separately consider internalization, measured by fluorescence

Received: January 7, 2019 Accepted: May 3, 2019 Published: May 3, 2019

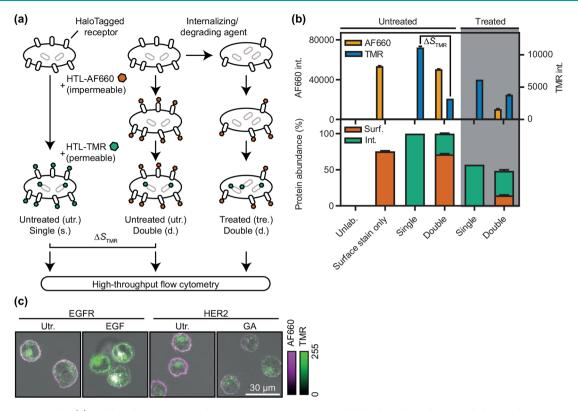


Figure 1. Assay principle. (a) Stable cell lines express the protein of interest genetically fused to the HaloTag. Labeling with permeable dye allows quantitation of total receptor (a, left column); sequential labeling with a cell-impermeable dye followed by a cell-permeable dye allows quantification of surface, internal, and total protein for hundreds of samples by high-throughput flow cytometry. Treated samples (a, right column) can then be compared to nontreated controls (a, middle column). (b) Typical data obtained from the assay performed as in (a), in this case for HER2. Top panel: Raw data with mean fluorescence intensities in channel-dependent, arbitrary units. Bottom panel: Data after rescaling. Error bars indicate 1 SD of duplicates. (c) Microscopy confirms localization-specific staining, allowing one to monitor induced internalization and degradation (Utr., untreated; GA, geldanamycin; EGF, epidermal growth factor).

or surface-specific biotinylation, and degradation by determining total protein levels via Western blot (WB).

In the simplest protocols, internalization is measured by using a fluorescently labeled affinity reagent against the molecule under study to quantify the amount of internalized receptor, again by acid washing off noninternalized ligand, compared to control samples that were incubated on ice. However, the timespan which can be observed in this manner is significantly limited because prolonged incubation on ice will eventually lead to cell death and cell permeabilization.

In a more sophisticated setup, which also allows one to determine recycling to the cell surface, a fluorescently labeled derivative of the ligand of interest has been used, and quenching antibodies can be added to distinguish surface-derived from intracellular signals in flow cytometry. To employ such an assay for screening again requires internalization-inhibited reference samples, in this case to correct for differences in quenching efficiency for different ligands. Furthermore, it involves the cumbersome work of labeling each and every binder fluorescently. This is even more difficult if one were to compare different classes of molecules, and for some small molecules, labeling may not even be possible at all without significantly affecting their structure and properties.

If the ligand carries a fluorescent label, its fate may be followed by flow cytometry or microscopy, but little to no knowledge regarding its effect on the target is gained in such a setup. Whether diminished surface fluorescence is due to "piggy-back" (passive) internalization of the affinity reagent

without changing the relevant rates or steady-state levels of the target, the inside—outside distribution of the target is affected, or whether even the total number of target molecules changes cannot be resolved. Furthermore, spurious and misleading fluorescent signals may be detected from cellular compartments to which the released dye localizes upon ligand degradation, in particular, if the remaining fluorescent label is cell-impermeable.

Whereas a myriad of techniques exist to label protein binders, few are suitable for visualizing the target directly on live cells for high-throughput applications, especially if the number as well as the location is of interest. 12 While the use of a labeled affinity reagent with a noncompeting epitope, such as an antibody, may appear to be a straightforward solution, <sup>10</sup> a suitable reagent—which does not alter the behavior and at the same time has sufficient affinity for the surface protein-may not always be available. For example, cross-linking by di- or multivalent detection reagents (e.g., secondary detection antibodies or streptavidin) may efficiently internalize surface proteins.<sup>13</sup> In early stages of drug development, the binding site for the entity of interest may also often not yet be known. Furthermore, the noncompeting binder or label may dissociate in a pH-dependent manner from the target at any time during recycling of the receptor and give rise to a sustained, falsepositive intracellular signal. Improved protocols based on indirect detection of the target, which aim to quantify surface and total protein at once, have been published. 14 However, they require detection with secondary antibodies, which may

be poorly quantitative, <sup>15</sup> and that cells remain impermeable during fixation, which we found not to be the case for several cell lines.

Total protein amounts have been routinely quantified by Western blots for decades. However, the throughput of the method is limited, and it provides no single-cell resolution. Moreover, by its semiquantitative nature, it is unclear how total protein measured by WB can be reliably related to surface and internal protein amounts.

Taken together, the presently available protocols to measure internalization and degradation do not yield true relative abundances of surface and internal (and therefore also total) target protein at once and are poorly scalable to high throughput.

Previous work utilizing the HaloTag (HT) technology has taken advantage of differential cell permeability of HaloTag ligands (HTLs) to resolve subcellular localization qualitatively in microscopy, demonstrating that a two-step labeling procedure enables binary distinction between two topological states, that is, the receptor being at the surface or internal. Based on these observations, we hypothesized that it may be possible to develop a high-throughput protocol that allows one to quantitatively measure both internalization and degradation.

The HaloTag protein is a 34 kDa engineered haloalkane dehalogenase, which can be genetically fused to a given protein of interest. <sup>18,19</sup> The tag enables covalent conjugation to HTLs, which combine a haloalkane, allowing irreversible and rapid covalent coupling to the HT, and a probe of choice, typically a fluorescent dye. It has furthermore been shown that by labeling of cytosolic protein—HT fusions with cell-permeable HTLs, protein degradation can be reliably monitored, <sup>20</sup> probably because the dye moiety is released by esterases upon HT degradation and subsequently diffuses out of the cell. <sup>18</sup>

Here, we present a homogeneous HaloTag-based, highthroughput surface protein internalization and degradation assay (SPIDA) protocol for labeling and direct quantification by multicolor flow cytometry. Furthermore, we show that a simple rescaling enables calculation of true relative abundances of surface and internally localized molecules, measured with different fluorophores. Using three test candidates, EGFR, HER2, and EpCAM, which are targets of directed cancer therapies approved for clinical application, <sup>21,22</sup> we demonstrate the robustness and generic applicability of our method in three stages: first, we validate the assay by direct comparison with conventional assays performed in parallel for well-studied inducers of internalization and degradation; second, we show that observations made with our assay agree well with data from the literature obtained with conventional assays; third, we apply the assay to previously unstudied molecules with high therapeutic potential.

## RESULTS AND DISCUSSION

**Method Outline.** We intended to develop a generic protocol to investigate large numbers of different molecules—potential inducers of internalization and degradation—in a straightforward and robust assay, which allows simultaneous quantification of internalization as well as degradation on a single-cell level over extended timeframes (Figure 1a). To this end, we generated different cell lines stably expressing an inducible HaloTag protein fusion with the surface protein of interest, based on the Flp-In T-Rex 293 system (Figure S-1, SI Methods). The Flp-In T-Rex 293 system allows one to generate stable cell lines expressing homogeneous levels of a

gene of interest under an inducible promoter from a single, well-transcribed genome integration site. The inducible system may be advantageous if sustained expression of the protein is toxic. We then took advantage of the fact that a HaloTag ligand conjugated to Alexa Fluor 660 (HTL-AF660) is completely cell-impermeable 19 at suitable concentrations, whereas the neutral HaloTag ligand bearing tetramethyl rhodamine (HTL-TMR) penetrates cells efficiently. Using a sequential double labeling protocol (see SI Methods for a detailed protocol), we exploited the differential permeability to quantify surface and internal protein simultaneously: First, HTL-AF660 is coupled exclusively to the protein of interest, which is present at the cell surface. Then, in the second step, the protein in intracellular stores is labeled with HTL-TMR, which can be detected in a separate channel (Figure 1b).

A straightforward rescaling based on untreated (utr.) control samples allows for calculation of relative abundances of internal, surface, and total receptor (SI Methods). In brief, the difference,  $\Delta S_{\rm TMR}$ , of normalized signals in the TMR channel is obtained by comparing single ( $S_{\rm TMR}(s.)$ ) labeling with TMR to the double ( $S_{\rm TMR}(d.)$ ) labeling (surface labeling with AF660 followed by TMR). This difference corresponds to the number of molecules blocked by the first, surface-specific step:

$$\Delta S_{\text{TMR}} = S_{\text{TMR}}(s.) - S_{\text{TMR}}(d.) = S_{\text{AF660,scaled}}(d.)$$
(1)

Here, the signal in the AF660 channel,  $S_{\rm AF660,scaled}({\rm d.})$ , is expressed in the units of the permeable dye TMR. It can be related to the actually measured intensity  $S_{\rm AF660}({\rm d.})$  by correction factor  $C_{\rm A}$ . By further setting the total amount of receptor of the untreated sample to 100%, it follows that

$$S_{AF660}(d.) \times C_A + S_{TMR}(d.) = S_{TMR}(s.) = 100\%$$
 (2)

This allows us to calculate  $C_A$  from the untreated sample, which can be used to obtain  $S_{AF660,scaled}(d.)$  (= $S_{AF660} \times C_A$ ) for all treated (and double-labeled) samples (Figure 1b,c).

In agreement with the literature,  $^{23,24}$  we observed that upon induction of protein expression in our HT-fusion cell lines, protein levels reached a steady state, which was maintained for at least 24 h (Figure S-2). This, in turn, further allowed us to add a time dimension to our assay in a simple manner by adding treatment agents at various time points and performing the final readout for all samples in parallel, with a nontreated reference sample corresponding to t = 0 h.

With our protocol, treatment and labeling can be applied to adherent cells in complete media. Thus, in contrast to other internalization protocols, the assay is homogeneous, does not involve prolonged incubation or treatment of detached cells, and can be performed without buffer exchange.

The presence of dead (and therefore permeable) cells is a severe issue for any internalization or recycling assay because, due to the loss of topological separation, all receptors will be accessible and thus appear to be at the surface (on the outside), even more so if the protein of interest is cytotoxic itself. In our protocol, this is addressed by simply including a commercially available fixable dead cell (permeability) staining step prior to cell fixation.

All experimental steps, including evaluation by flow cytometry, are very amenable to parallel processing in 96-well plates. We therefore provide a protocol which allowed us to routinely handle three or more such plates in a single experiment, allowing us to sample a total of  $\sim$ 400 data points with information from 1000 cells per time point (SI Methods).

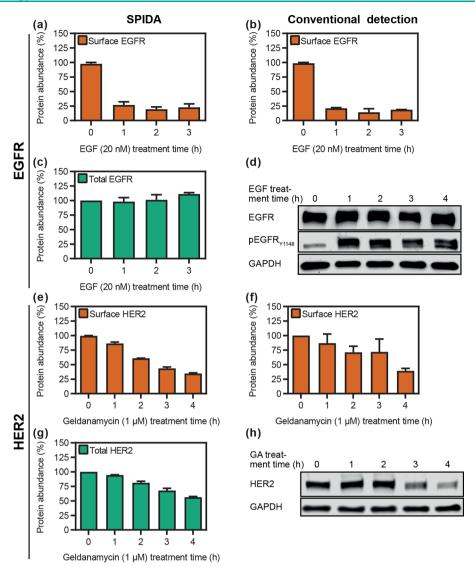


Figure 2. Comparison of SPIDA with conventional assays for surface protein internalization and degradation. Although SPIDA yields surface, internal, and total receptor levels in a single experiment, two separate experiments (typically flow cytometry and WB) are required in the conventional approach. (a—d) Surface levels of HT-EGFR after EGF treatment. Observation of surface levels by SPIDA (a) or conventional detection with a fluorescently labeled EGFR antibody (b) yields very similar results. Total levels as observed by SPIDA show a minor increase (c) and appear almost constant in WB (d). Note the rapid and robust phosphorylation of EGFR (Y1148) upon EGF treatment, expectedly coinciding with the internalization seen in (a,b) and indicating the functional integrity of HT-EGFR. (e—h) Surface and total levels of HT-HER2 after geldanamycin (GA) treatment. Surface levels of HT-HER2 after GA treatment as observed by SPIDA (e) and conventional detection with a fluorescently labeled monovalent anti-HER2 affibody (ZHER2) (g) decrease comparably, as do total levels according to SPIDA (g) or WB (h). Note that surface and internal values from SPIDA, originally representing the true relative abundance, were normalized to allow comparison with the conventional methods; bars indicate the grand mean of two fully independent experiments, with error bars indicating the standard error.

**Experimental Validation and Application of SPIDA** with Different Surface Proteins. We decided on three surface proteins, EGFR, HER2, and EpCAM, as test candidates to demonstrate the utility of our approach. After successful stable transfection of Flp-In T-REx 293 cells and isolation of single clones, these were analyzed for inducible expression by Western blot and flow cytometry. After induction, all clones showed expression to be inducible by at least a factor of 50 as judged by flow cytometry (Figure S-1a,b). Furthermore, blotted cell extracts revealed a specific band at the calculated size of the fusion protein for all clones (Figure S-1c).

To establish that SPIDA reliably measures induced surface protein internalization and degradation, we decided on two well-characterized phenomena: internalization of epidermal growth factor receptor (EGFR) upon binding of the cognate ligand epidermal growth factor (EGF)<sup>21</sup> and degradation of HER2 by geldanamycin (GA).<sup>25</sup> Whereas two separate experiments (typically flow cytometry and WB) are required in the conventional approaches to measure either surface or total protein levels, SPIDA yields surface, internal, and total receptor level in a single experiment. Thus, we replotted the SPIDA data for the EGF and GA treatments such that a direct comparison between the methods is possible (Figure 2).

**Epidermal Growth Factor Receptor (EGFR).** EGFR is a receptor tyrosine kinase (RTK) that is critically involved in the genesis of various types of cancer<sup>21,26</sup> and therefore a topic of active research into targeted therapies. EGFR internalization and degradation is triggered by intracellular phosphorylation upon ligand binding;<sup>27</sup> paradoxically, endocytosis of EGFR can regulate pro-tumorigenic signaling positively or negatively.<sup>28</sup>

We recorded the internalization kinetics upon EGF treatment with SPIDA (Figure 2a and Figure 3a), and in parallel, surface

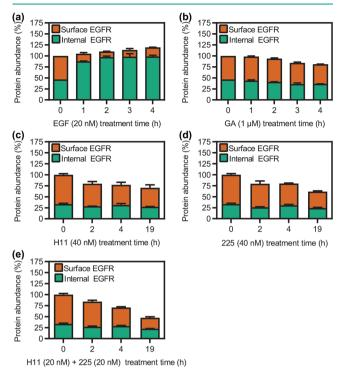


**Figure 3.** SPIDA measures internalization and degradation of EGFR. Using the HEK-TREx\_HT-EGFR cell line, we tested the effect of EGF (a; same data as in Figure 2a,c, but with relative abundances plotted) and geldanamycin (GA) (b). Furthermore, single mAbs H11 (c) and 225 (d) reduce EGFR levels only slightly, in agreement with the literature, <sup>11</sup> in contrast to their combination (e).

EGFR was detected by a noncompeting, directly labeled antibody (Figure 2b). To obtain also a reference for total protein levels (Figure 2c), we performed a WB (Figure 2d). As expected, HaloTagged EGFR was indeed efficiently internalized by 20 nM EGF, with excellent agreement between the SPIDA results and the reference protocol. After 2 h of exposure to 20 nM EGF, the fraction of surface receptor had dropped to 25% of the initial value for both setups. At the same time, internal protein levels increased from ~46 to ~88% (Figure 3a), an information only directly accessible through SPIDA. The carrier solution for EGF, containing bovine serum albumin (BSA), was inert (Figure S-3a). Overall, the results are also in good agreement with previously published data for HEK cells.<sup>29</sup> In addition, internalization kinetics have been reported to be merely slightly retarded by an N-terminal fusion to EGFR.<sup>30</sup> We observed a marked increase of Y1148 autophosphorylation (Figure 2d) of HaloTagged EGFR upon ligand stimulation, another indication that the functionality of EGFR is not impaired by the HaloTag fusion. We also noted that upon prolonged (4 h) EGF treatment, the total amount of EGFR increased slightly (Figure 2c and Figure 3a). This may, as it is correlated with intracellular receptor accumulation, be explained by saturation of the degradation machinery, in particular, considering the context of transiently induced strong overexpression.

Next, we looked at the effects of other treatments directed against EGFR and compared the results to data from the literature. Recent reports suggested that EGFR directly interacts with heat shock protein 90 (HSP90), and inhibition of HSP90 causes EGFR internalization and also degradation;<sup>31</sup> previous findings had indicated no interaction.<sup>32</sup> HSP90 inhibition is experimentally typically achieved by treatment with geldanamycin, a benzoquinone ansamycin,<sup>33</sup> which interferes with HSP90 substrate binding. In agreement with the current literature,<sup>31</sup> we observed a slow loss of surface EGFR upon treatment with GA (Figure 3b).

A combination of the murine parental antibody of cetuximab (mAb 225) and another EGFR antibody (H11) has been shown to down-regulate EGFR to at least ~50% remaining surface receptor in several cell lines. 11 Importantly, this occurs without the activation seen upon EGF treatment. 11 Therefore, we tested the single monoclonal antibodies (mAbs) (Figure 3c,d) and their combination (Figure 3e). In line with the reported results, we observed that the antibody combination effectively caused a sustained reduction of surface EGFR. Of note, the reduction in total EGFR was due to a loss of surface protein, whereas the internal receptor remained essentially constant—consistent with the proposed model of recycling inhibition by this antibody combination because the steadystate internal receptor level is only a function of synthesis and degradation rates. 11 We further noticed that the treatment significantly compromised cell health and increased the dead cell fraction, underlining the importance of a permeability parameter to exclude those cells from analysis for which topological separation of surface and internal receptor is lost (Figure S-3c).

Human Epidermal Growth Factor Receptor 2 (HER2). HER2 is another member of the EGFR family of RTKs, and its overexpression is known to be pivotal in the development of various types of cancer.<sup>35</sup> In contrast to EGFR, however, no ligand is known for HER2, and the extracellular domain constitutively adopts an open conformation in the absence of a ligand, resembling the ligand-bound state of other EGFR family members.<sup>36</sup> HER2 is assumed to only internalize very slowly under native conditions.<sup>37</sup> HER2 is well-known to be associated with HSP90, and it is only upon treatment with HSP90 inhibitors, like GA, that HER2 becomes susceptible to internalization and degradation.<sup>25</sup>

Again, for validation purposes, we first analyzed surface depletion of HER2 through GA by SPIDA (Figure 2e) and, in parallel, conventional surface detection by fluorescently labeled monovalent affibody ZHER2 (Figure 2f). For both methods, after 4 h, only approximately 50% of the initial total HER2 amount was still present (Figure 2g and Figure 4a), despite the noise in the conventional measurement being rather large compared to the SPIDA data. Using a classical WB from cell lysates, we also confirmed the reduction in total HER2 (Figure 2h). SPIDA additionally provides the levels of the remaining receptor: over 60% was localized on the inside of the cells after GA treatment, whereas in untreated cells, only ~30% was present intracellularly (Figure 4a).

In the past, there have been conflicting reports as to whether the degradation pathway of HER2 after GA treatment follows a lysosomal or proteasomal route. However, one current model assumes that a first proteasomal cleavage step enables the rapid internalization that precedes the degradation in the lysosome after GA treatment.<sup>37</sup> We have now used SPIDA to test this hypothesis. Indeed, proteasome inhibition with MG-132 rescued cells from GA treatment (Figure 4b), in line with previous results,<sup>14</sup> which had already shown rescue using lactacystin as a proteasomal inhibitor. MG-132 alone showed

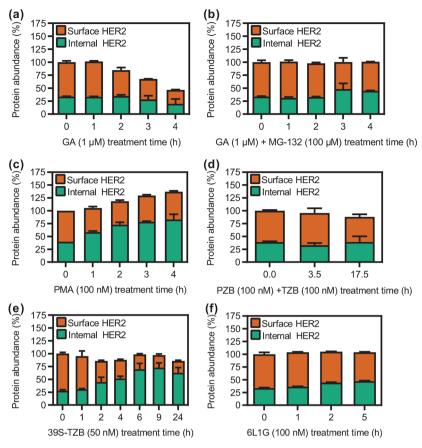


**Figure 4.** HER2 internalization and degradation investigated by SPIDA. HER2 is strongly degraded by GA (a; same data as in Figure 2e,g, but with relative abundances plotted) but rescued from degradation through the addition of proteasome inhibitor MG-132 (b). SPIDA confirms that PMA induces HER2 internalization but not degradation, in agreement with a recent report (c).<sup>34</sup> Combination of mAbs PZB and TZB (d) does not cause substantial receptor down-regulation, in contrast to 39S-TZB, which efficiently induces HER2 internalization, but only slow degradation (e). Biparatopic antitumor DARPins, which cause apoptosis,<sup>47</sup> leave the HER2 distribution mostly unaltered (f).

no effect on the HER2 amount or localization in 4 h (Figure S-4a). Together, these data are consistent with a model of an initial proteasomal cleavage within HER2, followed by internalization and lysosomal degradation.

In contrast to GA treatment, activation of the protein kinase C (PKC) upon phorbol 12-myristate 13-acetate (PMA) addition has recently been reported to cause internalization of HER2 without leading to degradation.<sup>34</sup> We observed PMA-treated cells for 4 h by SPIDA, and as recently published, HER2 was effectively internalized without degradation (Figure 4c), resulting in an increase of internal receptor from ~40% to more than 75% relative to the control. At the same time, because surface stores seem to at least partially be replenished after induced internalization in our induced overexpression system, an increase of total HER2 was observed in the first 2 h before plateauing out at around 130% of the initial value.

The FDA-approved mAb trastuzumab (TZB) binds domain IV of the HER2 ectodomain (HER2 ECD)<sup>35,38</sup> and was demonstrated to accumulate intracellularly before being slowly degraded, whereas the level of HER2 remains mostly unchanged during treatment of HER2-overexpressing cell lines.<sup>39,40</sup> The monoclonal antibody pertuzumab (PZB) binds domain II of the ECD, sterically interfering with heterodimerization,<sup>41</sup> and is also approved for treating HER2-positive cancers in a neoadjuvant setting.<sup>42</sup> Again, single treatment with PZB was shown to not significantly alter surface and total ErbB receptor levels.<sup>43</sup> In line with the

literature, we observed no noteworthy changes of the HER2 distribution after incubation with TZB or PZB alone in our assay (Figure S-4b,c).

It has been postulated that a combination of PZB and TZB (PZB+TZB), which shows synergistic antitumor activities and has been found efficacious in clinical application, <sup>44</sup> also acts through receptor down-regulation. <sup>43</sup> Although we have recently confirmed extensive receptor cross-linking by PZB +TZB (Stüber et al., manuscript in preparation), we found only a very modest reduction of total HER2 for PZB+TZB after 17.5 h (Figure 4d), which, in agreement with current literature, <sup>10</sup> emphasizes that HER2 degradation by PZB+TZB is a slow process.

In contrast, a biparatopic, tetravalent HER2 antibody, Medi4276, which is a fusion of a TZB scFv to the IgG 39S, has recently been reported to lead to rapid receptor internalization and degradation. We produced a closely similar molecule, by constructing the fusion of a TZB single-chain variable fragment (scFv) to the 39s IgG according to the publications, yielding 39S-TZB. Whereas strong receptor internalization by this construct was fully reproduced by our assay after exposing the cells to 50 nM of the antibody, we could not reproduce the report of a seemingly dramatic reduction in total HER2 after 24 h (Figure 4e) for our construct.

The antitumor biparatopic designed ankyrin repeat protein (DARPin)<sup>45</sup> 6L1G, which binds domains I and IV of two

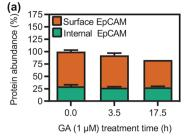
HER2 receptor molecules, 46 achieves a strong cytotoxic activity on HER2-dependent cancer cells<sup>47</sup> by interlocking and strongly immobilizing the receptors (Stüber et al., manuscript in preparation). For cells treated with 6L1G, we did, in line with previous studies, 47 observe no substantial change of the total amount (Figure 4f). It is noteworthy that in our HEK-TREx HT-HER2 cell line, HER2 overexpression is only transiently induced and these cells are not HER2addicted<sup>48</sup> and, consequently, not sensitive to treatment with molecules which specifically exploit HER2 addiction, such as DARPin 6L1G (Figure S-5). Thus, the induced receptor internalization and degradation are not caused by effects on receptor distribution, for example, through induction of apoptosis. We also tested whether the HER2-binding DARPin 6L1G, which has been shown to uncouple HER2 from EGFR, 47 affects EGFR levels. As expected, 6L1G did not alter the distribution of HT-EGFR (Figure S-3b).

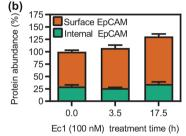
In summary, our HER2 data show that receptor crosslinking alone is not sufficient for efficient HER2 internalization or degradation. Our assay protocol may thus aid in future investigations into which precise geometric requirements of a binder—HER2 complex must be fulfilled in order to induce down-regulation of HER2.

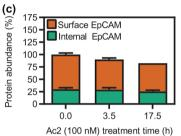
Epithelial Cell Adhesion Molecule (EpCAM). The epithelial cell adhesion molecule (EpCAM) is overexpressed on most tumors of epithelial origin and likely more accessible in tumors than in normal tissues.<sup>22</sup> It is further of particular interest for targeted therapy because it is also found on cancer stem cells.<sup>22</sup> In contrast to our previous examples, EpCAM is a rather small glycoprotein (~40 kDa)—roughly the same size as the HaloTag enzyme—and does not possess kinase activity. To our knowledge, for none of the EpCAM-targeting approaches described in the literature was it demonstrated that its uptake rate exceeds the rate of passive internalization through surface protein recycling; in other words, there is no evidence that any targeting ligand would induce internalization. Induction of EpCAM internalization and degradation would, however, be highly beneficial for targeting approaches for two reasons: First, direct inhibition of proliferation by down-regulation of EpCAM may be possible. 22 Second, massively increased EpCAM-specific uptake, possibly accompanied by an advantageous pharmacokinetic profile, could potentially enlarge the therapeutic window for treatment with drug-conjugated entities.

We therefore first explored whether EpCAM surface retention may also be abrogated by GA, as we observed for our two RTKs from the EGFR family. Not surprisingly, though, this was not the case for EpCAM (Figure 5a), for which no constitutive HSP90 interaction of the mature protein has been described in the literature. Ec1 and Ac2 are DARPins binding to different EpCAM epitopes, and both can act as targeting modules in several DARPin—toxin fusion formats with tunable pharmacokinetics. Whereas Ec1 mildly increased surface and total EpCAM (Figure 5b), it was slightly reduced by Ac2 (Figure 5c). A tetravalent DARPin construct obtained through inclusion of a self-associating leucine zipper domain, Ec1-LZ2-Ac2, also seemed to only mildly increase surface and total EpCAM (Figure 5d) in this HEK293 reporter line.

Together, our experiments with EpCAM-targeting DARPin constructs indicate that they only marginally alter the distribution of this surface protein. This suggests that screening for molecules that actively trigger EpCAM internalization or







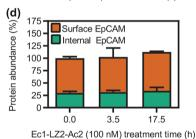


**Figure 5.** SPIDA with EpCAM. Whereas GA seems to cause only little surface EpCAM loss (a), EpCAM-binding DARPin Ec1 slightly increases surface EpCAM (b). In contrast, another DARPin, Ac2, causes minor EpCAM down-regulation (c). A tetravalent construct, in which both DARPins are combined, results in a very slight increase of surface EpCAM (d).

degradation, if they can be constructed, may generate more efficient EpCAM-targeting therapies, and this screening is readily possible with our protocol.

# CONCLUSIONS

Overall, we show through direct comparison with reference methods that SPIDA provides accurate results for surface, internal, and total receptor amounts from a single experiment, which can be generically scaled to high throughput. In addition to providing time resolution, SPIDA can be run for dozens of test ligands in parallel, without requiring their tedious labeling or the use of commercially available antibodies, which may often be only poorly characterized. <sup>52</sup> In contrast to approaches where affinity reagents are used for detection, all epitopes remain available on the protein of interest. As the HT is rather small (at least compared to antibodies) and attached through a long, flexible linker, it is much less likely to interfere with biological function or internalization and degradation of the

protein of interest than, for example, bivalent antibodies, as supported by the robust internalization and phosphorylation data of HT-EGFR upon EGF treatment that we report here.

Despite great advances in high-content screening by microscopy, a robust and informative analysis of subcellular localization, as well as total protein quantification, still requires advanced instrumentation and elaborate and extensive image processing. Although, in principle, our protocol can be adapted to readout by high-throughput microscopy, flow cytometry, which provides rapid and robust data evaluation, is fully sufficient because subcellular resolution is provided by means of localization-specific staining. Additional analysis dimensions could easily be added on modern multiparameter flow cytometers. We also observed that the SPIDA data were consistently less noisy than our and literature data obtained with affinity reagents.

The SPIDA principle could also be applied to similar tagligand systems (e.g., the SNAP<sup>55</sup> tag), given sufficient specificity of the (cell-permeable) ligands. Although we have established the methodology for HEK293 cells, we cannot exclude cell line-specific effects on the magnitude of induced receptor internalization and degradation. In the future, novel DNA editing tools may enable routine introduction of HaloTagged receptor fusions into disease model cell lines,<sup>56</sup> in turn allowing researchers to investigate cell-type and disorder-specific phenotypes regarding internalization and degradation.

We performed SPIDA successfully with two receptor tyrosine kinases of the epidermal growth factor family and an unrelated cell adhesion molecule and demonstrated that the effects of small molecules, growth factors, antibodies, as well as novel scaffold binders can all be robustly evaluated and directly compared. Established mechanisms, like EGFR internalization upon EGF treatment, down-regulation of HER2 by GA, degradation of EGFR by an antibody combination, and internalization of HER2 by 39S-TZB, could all be quantitatively observed in our system. Our data also show that HER2 down-regulation through the PZB+TZB combination is slow at best, but novel biparatopic agents are far more potent. This raises interesting questions about the exact requirements for rapid down-regulation that SPIDA may help to answer. Furthermore, our results with EpCAM indicate that the efficacy of current targeting approaches directed against this molecule may be potentiated if internalization and degradation can be induced, which can readily be measured by SPIDA. In summary, SPIDA provides a universally applicable protocol for drug discovery but also constitutes a quantitative basic research tool.

# ASSOCIATED CONTENT

### S Supporting Information

The Supporting Information is available free of charge on the ACS Publications website at DOI: 10.1021/acschembio.9b00016.

Additional methods including a detailed protocol for SPIDA, further data regarding protein expression and labeling in the HEK-TREx cell lines, SPIDA of EGFR and HER2, and a cell proliferation assay for HEK-TREx\_HT-HER2, presented in Figures S1–S5 (PDF)

#### AUTHOR INFORMATION

# **Corresponding Author**

\*E-mail: plueckthun@bioc.uzh.ch. Fax: +41-44-63 557 12.

#### ORCID ®

Andreas Plückthun: 0000-0003-4191-5306

#### **Author Contributions**

J.C.S. and F.K. contributed equally to this work. J.C.S., F.K., and A.P. designed the research and analyzed the data. J.C.S. and F.K. performed the experiments. J.C.S., F.K., and A.P. wrote the paper.

#### **Funding**

Funding was obtained by the Schweizerischer Nationalfonds, Grant No. 310030B 166676, to A.P.

#### Notes

The authors declare no competing financial interest.

#### ACKNOWLEDGMENTS

F. Brandl and H. Merten are kindly acknowledged for providing the EpCAM binding DARPins and the plasmid for the EpCAM leucine zipper fusion. We thank C. Kunz and M. Enzelberger (Morphosys) for the pYMex10 plasmid, and U. Zangemeister-Wittke for supplying pertuzumab. Flow cytometry and imaging were performed with equipment maintained by the Flow Cytometry Facility (FCF) and the Center for Microscopy and Image Analysis (ZMB), respectively, of the University of Zurich.

#### REFERENCES

- (1) Sachdev, D., Singh, R., Fujita-Yamaguchi, Y., and Yee, D. (2006) Down-regulation of insulin receptor by antibodies against the type i insulin-like growth factor receptor: Implications for anti-insulin-like growth factor therapy in breast cancer. *Cancer Res.* 66, 2391–2402.
- (2) Nollet, M., Stalin, J., Moyon, A., Traboulsi, W., Essaadi, A., Robert, S., Malissen, N., Bachelier, R., Daniel, L., Foucault-Bertaud, A., Gaudy-Marqueste, C., Lacroix, R., Leroyer, A. S., Guillet, B., Bardin, N., Dignat-George, F., and Blot-Chabaud, M. (2017) A novel anti-CD146 antibody specifically targets cancer cells by internalizing the molecule. *Oncotarget 8*, 112283–112296.
- (3) Sievers, E. L., and Senter, P. D. (2013) Antibody-drug conjugates in cancer therapy. *Annu. Rev. Med.* 64, 15–29.
- (4) Kontermann, R. E., and Brinkmann, U. (2015) Bispecific antibodies. *Drug Discovery Today* 20, 838-847.
- (5) Carter, P. J., and Lazar, G. A. (2017) Next generation antibody drugs: Pursuit of the 'high-hanging fruit'. *Nat. Rev. Drug Discovery* 17, 197–223
- (6) Lagerström, M. C., and Schiöth, H. B. (2008) Structural diversity of G protein-coupled receptors and significance for drug discovery. *Nat. Rev. Drug Discovery 7*, 339–357.
- (7) Lai, A. C., and Crews, C. M. (2017) Induced protein degradation: An emerging drug discovery paradigm. *Nat. Rev. Drug Discovery* 16, 101–114.
- (8) Honegger, A. M., Dull, T. J., Felder, S., Van Obberghen, E., Bellot, F., Szapary, D., Schmidt, A., Ullrich, A., and Schlessinger, J. (1987) Point mutation at the ATP binding site of EGF receptor abolishes protein-tyrosine kinase activity and alters cellular routing. *Cell* 51, 199–209.
- (9) Jeong, J., VanHouten, J. N., Dann, P., Kim, W., Sullivan, C., Yu, H., Liotta, L., Espina, V., Stern, D. F., Friedman, P. A., and Wysolmerski, J. J. (2016) PMCA2 regulates HER2 protein kinase localization and signaling and promotes HER2-mediated breast cancer. *Proc. Natl. Acad. Sci. U. S. A. 113*, E282–E290.
- (10) Li, J. Y., Perry, S. R., Muniz-Medina, V., Wang, X., Wetzel, L. K., Rebelatto, M. C., Masson Hinrichs, M. J., Bezabeh, B. Z., Fleming, R. L., Dimasi, N., Feng, H., Toader, D., Yuan, A. Q., Xu, L., Lin, J., Gao, C., Wu, H., Dixit, R., Osbourn, J. K., and Coats, S. R. (2016) A

biparatopic HER2-targeting antibody-drug conjugate induces tumor regression in primary models refractory to or ineligible for HER2-targeted therapy. *Cancer Cell* 29, 117–129.

- (11) Spangler, J. B., Neil, J. R., Abramovitch, S., Yarden, Y., White, F. M., Lauffenburger, D. A., and Wittrup, K. D. (2010) Combination antibody treatment down-regulates epidermal growth factor receptor by inhibiting endosomal recycling. *Proc. Natl. Acad. Sci. U. S. A. 107*, 13252–13257.
- (12) Hinner, M. J., and Johnsson, K. (2010) How to obtain labeled proteins and what to do with them. *Curr. Opin. Biotechnol.* 21, 766–776.
- (13) Zhu, W., Okollie, B., and Artemov, D. (2007) Controlled internalization of Her-2/neu receptors by cross-linking for targeted delivery. *Cancer Biol. Ther.* 6, 1960–1966.
- (14) Lerdrup, M., Hommelgaard, A. M., Grandal, M., and Van Deurs, B. (2006) Geldanamycin stimulates internalization of ErbB2 in a proteasome-dependent way. *J. Cell Sci.* 119, 85–95.
- (15) Müller, K. M., Arndt, K. M., and Plückthun, A. (1998) Model and simulation of multivalent binding to fixed ligands. *Anal. Biochem.* 261, 149–158.
- (16) Svendsen, S., Zimprich, C., McDougall, M. G., Klaubert, D. H., and Los, G. V. (2008) Spatial separation and bidirectional trafficking of proteins using a multi-functional reporter. *BMC Cell Biol.* 9, 17.
- (17) Ai, X., Fischer, P., Palyha, O. C., Wisniewski, D., Hubbard, B., Akinsanya, K., Strack, A. M., and Ehrhardt, A. G. (2013) Utilizing HaloTag technology to track the fate of PCSK9 from intracellular vs. extracellular sources. *Curr. Chem. Genomics* 6, 38–47.
- (18) Los, G. V., Encell, L. P., McDougall, M. G., Hartzell, D. D., Karassina, N., Zimprich, C., Wood, M. G., Learish, R., Ohana, R. F., Urh, M., Simpson, D., Mendez, J., Zimmerman, K., Otto, P., Vidugiris, G., Zhu, J., Darzins, A., Klaubert, D. H., Bulleit, R. F., and Wood, K. V. (2008) HaloTag: A novel protein labeling technology for cell imaging and protein analysis. *ACS Chem. Biol.* 3, 373–382.
- (19) Hirata, T., Terai, T., Yamamura, H., Shimonishi, M., Komatsu, T., Hanaoka, K., Ueno, T., Imaizumi, Y., Nagano, T., and Urano, Y. (2016) Protein-coupled fluorescent probe to visualize potassium ion transition on cellular membranes. *Anal. Chem.* 88, 2693–2700.
- (20) Yamaguchi, K., Inoue, S., Ohara, O., and Nagase, T. (2009) in Reverse chemical genetics: Methods and protocols (Koga, H., Ed.), pp 121–131, Humana Press, Totowa, NJ.
- (21) Yarden, Y., and Pines, G. (2012) The ErbB network: At last, cancer therapy meets systems biology. Nat. Rev. Cancer 12, 553–563.
- (22) Simon, M., Stefan, N., Plückthun, A., and Zangemeister-Wittke, U. (2013) Epithelial cell adhesion molecule-targeted drug delivery for cancer therapy. *Expert Opin. Drug Delivery* 10, 451–468.
- (23) Xiao, S., White, J. F., Betenbaugh, M. J., Grisshammer, R., and Shiloach, J. (2013) Transient and stable expression of the neurotensin receptor NTS1: A comparison of the baculovirus-insect cell and the T-Rex-293 expression systems. *PLoS One 8*, No. e63679.
- (24) Chruścicka, B., Burnat, G., Brański, P., Chorobik, P., Lenda, T., Marciniak, M., and Pilc, A. (2015) Tetracycline-based system for controlled inducible expression of group iii metabotropic glutamate receptors. *J. Biomol. Screening* 20, 350–358.
- (25) Miller, P., DiOrio, C., Moyer, M., Schnur, R. C., Bruskin, A., Cullen, W., and Moyer, J. D. (1994) Depletion of the *ErbB*-2 gene product p185 by benzoquinoid ansamycins. *Cancer Res.* 54, 2724–2730.
- (26) Kovacs, E., Zorn, J. A., Huang, Y., Barros, T., and Kuriyan, J. (2015) A structural perspective on the regulation of the EGF receptor. *Annu. Rev. Biochem.* 84, 739–764.
- (27) Levkowitz, G., Waterman, H., Zamir, E., Kam, Z., Oved, S., Langdon, W. Y., Beguinot, L., Geiger, B., and Yarden, Y. (1998) C-Cbl/Sli-1 regulates endocytic sorting and ubiquitination of the epidermal growth factor receptor. *Genes Dev.* 12, 3663–3674.
- (28) Tomas, A., Futter, C. E., and Eden, E. R. (2014) EGF receptor trafficking: Consequences for signaling and cancer. *Trends Cell Biol.* 24, 26–34.

- (29) Carter, R. E., and Sorkin, A. (1998) Endocytosis of functional epidermal growth factor receptor-green fluorescent protein chimera. *J. Biol. Chem.* 273, 35000–35007.
- (30) Liu, P., Sudhaharan, T., Koh, R. M. L., Hwang, L. C., Ahmed, S., Maruyama, I. N., and Wohland, T. (2007) Investigation of the dimerization of proteins from the epidermal growth factor receptor family by single wavelength fluorescence cross-correlation spectroscopy. *Biophys. J.* 93, 684–698.
- (31) Ahsan, A., Ramanand, S. G., Whitehead, C., Hiniker, S. M., Rehemtulla, A., Pratt, W. B., Jolly, S., Gouveia, C., Truong, K., Waes, C. V., Ray, D., Lawrence, T. S., and Nyati, M. K. (2012) Wild-type EGFR is stabilized by direct interaction with Hsp90 in cancer cells and tumors. *Neoplasia*. 14, 670–677.
- (32) Citri, A., Gan, J., Mosesson, Y., Vereb, G., Szollosi, J., and Yarden, Y. (2004) Hsp90 restrains ErbB-2/HER2 signalling by limiting heterodimer formation. *EMBO Rep.* 5, 1165–1170.
- (33) Stebbins, C. E., Russo, A. A., Schneider, C., Rosen, N., Hartl, F. U., and Pavletich, N. P. (1997) Crystal structure of an Hsp90-geldanamycin complex: Targeting of a protein chaperone by an antitumor agent. *Cell* 89, 239–250.
- (34) Dietrich, M., Malik, M. S., Nikolaysen, F., Skeie, M., and Stang, E. (2018) Protein kinase C mediated internalization of ErbB2 is independent of clathrin, ubiquitination and Hsp90 dissociation. *Exp. Cell Res.* 371, 139–150.
- (35) Roskoski, R., Jr. (2014) The ErbB/HER family of protein-tyrosine kinases and cancer. *Pharmacol. Res.* 79, 34–74.
- (36) Jost, C., Stüber, J. C., Honegger, A., Wu, Y., Batyuk, A., and Plückthun, A. (2017) Rigidity of the extracellular part of HER2: Evidence from engineering subdomain interfaces and shared-helix darpin-darpin fusions. *Protein Sci.* 26, 1796–1806.
- (37) Bertelsen, V., and Stang, E. (2014) The mysterious ways of ErbB2/HER2 trafficking. *Membranes* 4, 424–46.
- (38) Cho, H. S., Mason, K., Ramyar, K. X., Stanley, A. M., Gabelli, S. B., Denney, D. W., Jr, and Leahy, D. J. (2003) Structure of the extracellular region of HER2 alone and in complex with the Herceptin Fab. *Nature* 421, 756–60.
- (39) Austin, C. D., De Mazière, A. M., Pisacane, P. I., Van Dijk, S. M., Eigenbrot, C., Sliwkowski, M. X., Klumperman, J., and Scheller, R. H. (2004) Endocytosis and sorting of ErbB2 and the site of action of cancer therapeutics trastuzumab and geldanamycin. *Mol. Biol. Cell* 15, 5268–5282.
- (40) Ram, S., Kim, D., Ober, R. J., and Ward, E. S. (2014) The level of HER2 expression is a predictor of antibody-HER2 trafficking behavior in cancer cells. *Mabs.* 6, 1211–1219.
- (41) Franklin, M. C., Carey, K. D., Vajdos, F. F., Leahy, D. J., De Vos, A. M., and Sliwkowski, M. X. (2004) Insights into ErbB signaling from the structure of the ErbB2-pertuzumab complex. *Cancer Cell S*, 317–328.
- (42) Amiri-Kordestani, L., Wedam, S., Zhang, L., Tang, S., Tilley, A., Ibrahim, A., Justice, R., Pazdur, R., and Cortazar, P. (2014) First FDA approval of neoadjuvant therapy for breast cancer: pertuzumab for the treatment of patients with HER2-positive breast cancer. *Clin. Cancer Res.* 20, 5359–5364.
- (43) Nahta, R., Hung, M.-C., and Esteva, F. J. (2004) The HER2-targeting antibodies trastuzumab and pertuzumab synergistically inhibit the survival of breast cancer cells. *Cancer Res.* 64, 2343–2346.
- (44) Von Minckwitz, G., Procter, M., De Azambuja, E., Zardavas, D., Benyunes, M., Viale, G., Suter, T., Arahmani, A., Rouchet, N., Clark, E., Knott, A., Lang, I., Levy, C., Yardley, D. A., Bines, J., Gelber, R. D., Piccart, M., and Baselga, J. (2017) Adjuvant pertuzumab and trastuzumab in early HER2-positive breast cancer. *N. Engl. J. Med.* 377, 122–131.
- (45) Plückthun, A. (2015) Designed ankyrin repeat proteins (DARPins): Binding proteins for research, diagnostics, and therapy. *Annu. Rev. Pharmacol. Toxicol.* 55, 489–511.
- (46) Epa, V. C., Dolezal, O., Doughty, L., Xiao, X., Jost, C., Plückthun, A., and Adams, T. E. (2013) Structural model for the interaction of a designed ankyrin repeat protein with the human epidermal growth factor receptor 2. *PLoS One 8*, No. e59163.

(47) Tamaskovic, R., Schwill, M., Nagy-Davidescu, G., Jost, C., Schaefer, D. C., Verdurmen, W. P. R., Schaefer, J. V., Honegger, A., and Plückthun, A. (2016) Intermolecular biparatopic trapping of ErbB2 prevents compensatory activation of PI3K/AKT via Ras-p110 crosstalk. *Nat. Commun.* 7, 11672.

- (48) Carey, L. A. (2012) HER2—a good addiction. Nat. Rev. Clin. Oncol. 9, 196.
- (49) Simon, M., Stefan, N., Borsig, L., Plückthun, A., and Zangemeister-Wittke, U. (2014) Increasing the antitumor effect of an EpCAM-targeting fusion toxin by facile click PEGylation. *Mol. Cancer Ther.* 13, 375–385.
- (50) Stefan, N., Zimmermann, M., Simon, M., Zangemeister-Wittke, U., and Plückthun, A. (2014) Novel prodrug-like fusion toxin with protease-sensitive bioorthogonal PEGylation for tumor targeting. *Bioconjugate Chem.* 25, 2144–2156.
- (51) Stefan, N., Martin-Killias, P., Wyss-Stoeckle, S., Honegger, A., Zangemeister-Wittke, U., and Plückthun, A. (2011) DARPins recognizing the tumor-associated antigen EpCAM selected by phage and ribosome display and engineered for multivalency. *J. Mol. Biol.* 413, 826–843.
- (52) Bradbury, A., and Plückthun, A. (2015) Reproducibility: Standardize antibodies used in research. *Nature 518*, 27–29.
- (53) Boutros, M., Heigwer, F., and Laufer, C. (2015) Microscopy-based high-content screening. *Cell* 163, 1314–1325.
- (54) Haasen, D., Schnapp, A., Valler, M. J., and Heilker, R. (2006) G protein-coupled receptor internalization assays in the high-content screening format. *Methods Enzymol.* 414, 121–139.
- (55) Sun, X., Zhang, A., Baker, B., Sun, L., Howard, A., Buswell, J., Maurel, D., Masharina, A., Johnsson, K., Noren, C. J., Xu, M.-Q., and Corrêa, I. R. (2011) Development of SNAP-tag fluorogenic probes for wash-free fluorescence imaging. *ChemBioChem* 12, 2217–2226.
- (56) Fellmann, C., Gowen, B. G., Lin, P.-C., Doudna, J. A., and Corn, J. E. (2017) Cornerstones of CRISPR-Cas in drug discovery and therapy. *Nat. Rev. Drug Discovery* 16, 89.